

A gaseous metal disk around a white dwarf

B.T. Gänsicke¹, T.R. Marsh¹, J. Southworth¹, A. Rebassa-Mansergas¹

¹ Department of Physics, University of Warwick, Coventry CV4 7AL, UK

The destiny of planetary systems through the late evolution of their host stars is very uncertain. We report a metal-rich gas disk around a moderately hot and young white dwarf. A dynamical model of the double-peaked emission lines constrains the outer disk radius to just 1.2 solar radii. The likely origin of the disk is a tidally disrupted asteroid, which has been destabilised from its initial orbit at a distance of more than 1000 solar radii by the interaction with a relatively massive planetesimal object or a planet. The white dwarf mass of 0.77 solar masses implies that planetary systems may form around high-mass stars.

White dwarfs are the compact end products of stars with masses up to ~ 8 solar masses (1). Because of the low luminosity of white dwarfs the detection of low mass stellar companions (2) or planets (3) is much easier around white dwarfs than around main sequence stars. During a search for cool companions to white dwarfs, an infrared excess was discovered around the white dwarf G29–38 (4). The atmosphere of G29–38 has been found to be enriched with metals, i.e. elements heavier than helium. The sedimentation time scales of heavy elements in the high-gravity atmospheres of white dwarfs are short compared to the evolutionary time scale of these stars (5) and, hence, the high metal abundances in G29–38 imply that this star is accreting at a relatively high rate (6). Deep imaging and asteroseismological studies of G29–38 ruled out a brown dwarf companion (7, 8) and led to the hypothesis of a cool dust cloud around the

white dwarf. The presence of dust near G29–38 has been verified by infrared observations with the Spitzer Space Telescope (9). Infrared surveys of white dwarfs exhibiting metal enriched atmospheres recently led to the discovery of three other potential dust disks (10, 11, 12). A possible origin of such dust disks is the tidal disruption of either comets (13) or asteroids (14). Asteroids appear to be more likely candidates as they can explain the large amount of metals accreted by the white dwarfs from the dusty environment as well as the absence of hydrogen or helium. While the detection of asteroid debris around G29–38 and the other white dwarfs represents a possible link to the existence of planetary systems around their main-sequence progenitors stars, modelling the excess infrared luminosity provides no direct information on the geometric location and extension of the dust, impeding a more detailed understanding of the nature and origin of the circumstellar material (9). A concentration of dust in the equatorial plane around G29–38 has been suggested on the basis of the relative amplitudes of non-radial white dwarf pulsations observed in the optical and infrared wavebands (7).

We identified SDSS J122859.93+104032.9 as a moderately hot white dwarf in the Data Release 4 of the Sloan Digital Sky Survey (SDSS) (15), but noted very unusual emission lines of the Ca II 850-866 nm triplet, as well as weaker emission lines of Fe II at 502 nm and 517 nm. The line profiles of the Ca II triplet display a distinct double-peaked morphology, which is the common hallmark of a gaseous, rotating disk (16, 4). Time-resolved spectroscopy (Fig. 1) and photometry do not reveal any radial velocity or brightness variations. These data exclude the possibility that SDSS 1228+1040 is an interacting white dwarf binary, in which an accretion disk around the white dwarf forms from material supplied by a nearby companion star. Furthermore, the absence of Balmer and helium emission lines implies that the gaseous disk around SDSS 1228+1040 must be extremely deficient in volatile elements, which independently rules out an interacting binary nature for this object.

Our detection of double-peaked metal emission lines from a circumstellar disk in SDSS 1228+1040

provides direct evidence for hydrogen and helium depleted material rotating around a white dwarf at a very short distance in a flat disk-like structure. Assuming that the Ca II line profiles (Fig. 1) originate indeed in a circumstellar disk, it must have an azimuthal asymmetry to match the asymmetry in the profiles. Such asymmetries are known in the disks around B-type emission line stars (Be stars) (2). Drawing upon this analogy, we developed a dynamical model of the Ca II line profiles (Fig. 3, SOM Sect. 1), which provides a robust constraint on the outer radius of the disk of $\simeq 1.2$ solar radii.

As the main-sequence stars hosting planetary systems evolve through the red giant stage, they swell up in radius and destroy planets and asteroids out to many hundred solar radii (19). The white dwarf mass of SDSS 1228+1040 implies a relatively massive main sequence progenitor of $\sim 4 - 5$ solar masses (20), which will have expanded to a radius of ~ 1000 solar radii (21). It is therefore impossible that the material making up the present-day disk has survived the giant phase at its current location, and must instead have been brought inwards from outside a distance of 1000 solar radii. Planetary debris which migrated outwards to large radii during the giant phase is expected to have relatively stable orbits unless perturbed by larger-mass objects (13). A likely scenario is therefore that one or more planets which survived the evolution of the progenitor of SDSS 1228+1040 destabilised the orbit of an asteroid at some point after the end of the planetary nebula phase. Getting close enough to the compact star, the asteroid is tidally disrupted, forming a disk of metal-rich debris which subsequently sublimates in the radiation field of the white dwarf. The radius derived from our dynamical model is in fact compatible with the tidal disruption radius for a rocky asteroid (22).

A strong Mg II 448 nm absorption line is detected in the spectrum of the white dwarf and implies a magnesium abundance in its atmosphere comparable to that of the Sun. This is extremely unusual for white dwarfs, which typically have pristine hydrogen atmospheres. The large abundance of magnesium can only be explained by sustained accretion, as the diffusion

time scale for magnesium in a white dwarf atmosphere of 22 000 K (Fig. 2, Table 1) is only ~ 5 days (23). Moreover, the accreted material must be of very low helium abundance, as already small traces of helium mixed into the radiative atmosphere of the white dwarf would cause noticeable He I 447 nm absorption, which is not observed. The absence of helium lines in the white dwarf spectrum places an upper limit on the helium abundance of the material accreted from the circumstellar disc of 0.1 times the solar value, which is an independent evidence for a metal-rich composition of the disk around SDSS 1228+1040.

No infrared excess has been found around metal-polluted white dwarfs hotter than 15 000 K (12), which suggests that the radiation field of these hot white dwarfs causes sublimation of a dust disk. The case of SDSS 1228+1040 demonstrates that planetary debris material can be detected around younger and hotter white dwarfs in the form of gaseous disks. Prompted by the discovery of SDSS 1228+1040, we have inspected 406 SDSS spectra of white dwarfs with hydrogen dominated atmospheres brighter than $g = 17.5$ that are contained in the SDSS Data Release 4 (7), and find just one additional object which potentially exhibits flux excess in the region of the Ca II triplet (SDSSJ104341.53+085558.2, Fig. S1), so SDSS 1228+1040 is clearly a rare object. The detection of a metal-rich debris disk around this relatively massive white dwarf indicates that the formation of planetary systems can take place also around short-lived massive stars.

References and Notes

1. P. D. Dobbie, *et al.*, *MNRAS* **369**, 383 (2006).
2. J. Farihi, E. E. Becklin, B. Zuckerman, *ApJS* **161**, 394 (2005).
3. M. R. Burleigh, F. J. Clarke, S. T. Hodgkin, *MNRAS* **331**, L41 (2002).
4. B. Zuckerman, E. E. Becklin, *Nat* **330**, 138 (1987).

5. C. Paquette, C. Pelletier, G. Fontaine, G. Michaud, *ApJS* **61**, 177 (1986).
6. D. Koester, J. Provencal, H. L. Shipman, *A&A* **320**, L57 (1997).
7. J. R. Graham, K. Matthews, G. Neugebauer, B. T. Soifer, *ApJ* **357**, 216 (1990).
8. M. J. Kuchner, C. D. Koresko, M. E. Brown, *ApJ Lett.* **508**, L81 (1998).
9. W. T. Reach, *et al.*, *ApJ Lett.* **635**, L161 (2005).
10. E. E. Becklin, *et al.*, *ApJ Lett.* **632**, L119 (2005).
11. M. Kilic, T. von Hippel, S. K. Leggett, D. E. Winget, *ApJ Lett.* **632**, L115 (2005).
12. M. Kilic, T. von Hippel, S. K. Leggett, D. E. Winget, *ApJ* **646**, 474 (2006).
13. J. H. Debes, S. Sigurdsson, *ApJ* **572**, 556 (2002).
14. M. Jura, *ApJ Lett.* **584**, L91 (2003).
15. J. K. Adelman-McCarthy, *et al.*, *ApJS* **162**, 38 (2006).
16. P. Young, D. P. Schneider, S. A. Shectman, *ApJ* **245**, 1035 (1981).
17. K. Horne, T. R. Marsh, *MNRAS* **218**, 761 (1986).
18. A. Meilland, P. Stee, J. Zorec, S. Kanaan, *A&A* **455**, 953 (2006).
19. I.-J. Sackmann, A. I. Boothroyd, K. E. Kraemer, *ApJ* **418**, 457 (1993).
20. T. Blöcker, *A&A* **299**, 755 (1995).
21. J. R. Hurley, O. R. Pols, C. A. Tout, *MNRAS* **315**, 543 (2000).
22. B. J. R. Davidsson, *Icarus* **142**, 525 (1999).

23. D. Koester, D. Wilken, *A&A* **453**, 1051 (2006).
24. D. J. Eisenstein, *et al.*, *ApJS* **in press**, [astro-ph/0606700](#) (2006).
25. I. Hubeny, T. Lanz, *ApJ* **439**, 875 (1995).
26. Acknowledgements BTG, TRM, JS, and ARM have been supported by PPARC in form of an Advanced Fellowship, a Senior Research Fellowship, a postdoctoral grant, and a joint PPARC-IAC studentship. The observations were obtained at the Spanish Observatorio del Roque de los Muchachos of the Instituto de Astrofísica de Canarias using the William Herschel Telescope and Isaac Newton Telescope. We thank Peter Wheatley for constructive criticism on the manuscript, Detlev Koester for discussions on diffusion time scales, and Ivan Hubeny for his ongoing support of the TLUSTY/SYNSPEC codes.

Funding for the SDSS and SDSS-II has been provided by the Alfred P. Sloan Foundation, the Participating Institutions, the National Science Foundation, the U.S. Department of Energy, the National Aeronautics and Space Administration, the Japanese Monbukagakusho, the Max Planck Society, and the Higher Education Funding Council for England. The SDSS Web Site is <http://www.sdss.org/>.

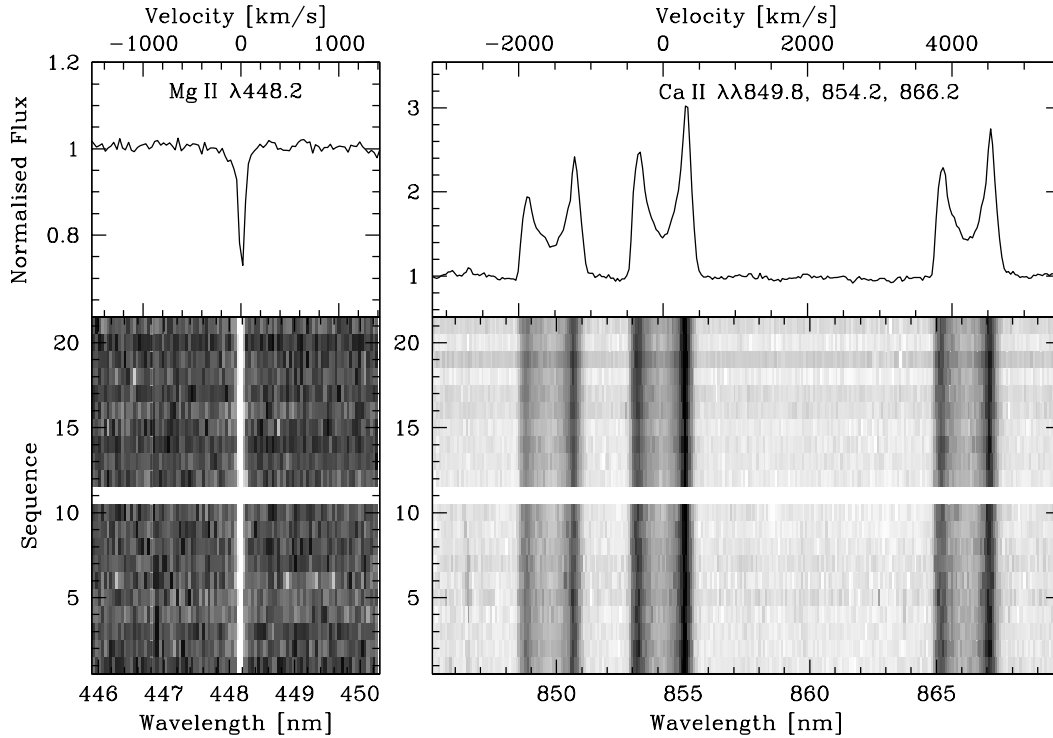


Fig. 1. Time-resolved spectroscopy of SDSS 1228+1040. Medium resolution spectroscopy of SDSS 1228+1040 was obtained with the double-arm spectrograph ISIS on the 4.2m William Herschel Telescope on La Palma. Two sets of ten consecutive spectra each were obtained on June 30 2006 and July 1 2006. The exposure times of the individual spectra were 600 s. The bottom panel shows the two time-series of spectra, each extending over 1.7 h, centered on the calcium emission triplet (right) and the magnesium absorption line (left). The normalised average spectra are shown in the top panels. Radial velocities are given in the upper axes with respect to Ca II 854 nm (left) and Mg II 448 nm (right). The radial velocity of the Mg II line is stable to within ± 4 km/s over time scales of 20 min to one day. Additional time-series photometry obtained at the Isaac Newton Telescope shows the star at constant brightness within ± 0.01 mag.

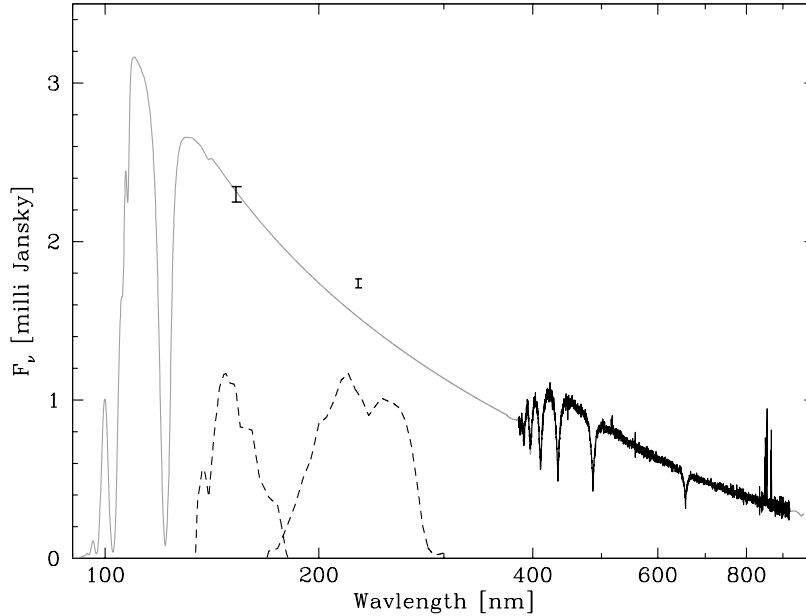


Fig. 2. A model of the white dwarf in SDSS 1228+1040. The optical SDSS spectrum of SDSS 1228+1040 is plotted in black. In addition to the Ca II emission lines seen in Fig. 1, also Fe II 517 nm (and 502 nm, not visible at the plotted scale) is detected. The signal-to-noise ratio of the iron lines is too low to assess the shape of their profiles. The insets display blow-ups of the H β 486 nm, H γ 434 nm, and H δ 410 nm Balmer lines and the Mg II 448 nm absorption line. The observed spectrum has been modelled with synthetic white dwarf spectra (25), resulting in an effective temperature of $T_{\text{WD}} = 22\,020 \pm 120$ K, a surface gravity of $\log g = 8.24 \pm 0.04$, an abundance of Mg II of 0.8 ± 0.15 with respect to solar abundances, and a limit of $v \sin i \leq 20$ km/s on the rotation rate of the white dwarf. The best-fit white dwarf model is plotted in gray. The ultraviolet fluxes detected by GALEX (<http://galex.stsci.edu/GR2/>) are indicated as black error bars, the filter transmission curves of GALEX are shown by dashed lines. The best-fit white dwarf model is consistent with the far-ultraviolet GALEX flux, but a flux excess is observed in the near-ultraviolet. A host of Fe II transitions lies within the near-ultraviolet bandpass (6), and could be in emission in SDSS 1228+1040, explaining the observed flux excess.

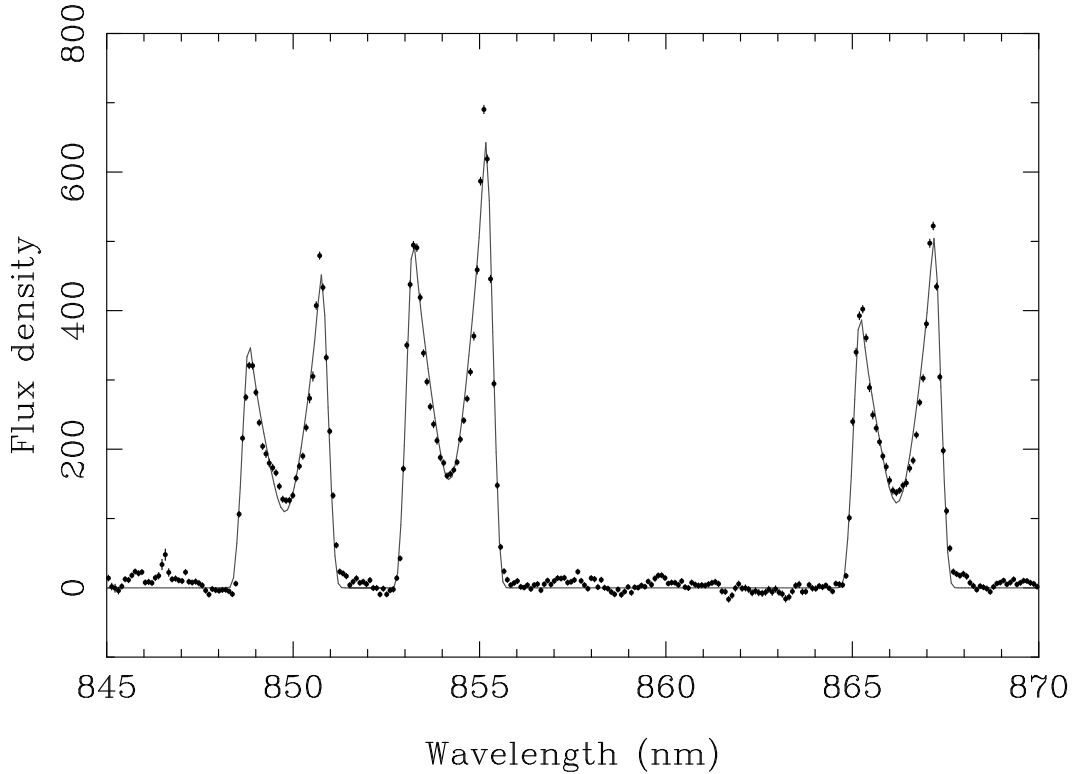


Fig. 3. A dynamical debris disk model. We modelled the observed Ca II emission line profiles (points) by assuming that the orbits in the disk took the form of a series of co-aligned elliptical orbits of constant eccentricity (see SOM Sect. 1). We find an outer radius of 1.2 solar radii for an edge-on disk and an ellipticity of 0.021. The measured outer radius of the disk is relatively invulnerable to the detailed assumptions of the model as it is primarily fixed by the velocities of the emission line peaks. The value given has to be interpreted as an upper limit since the radius scales as $\sin^2 i$ for disks inclined by angle i to the line of sight. The deep central dips of the profiles imply optically thick emission (4) and suggest that the orbital inclination must be quite high, $> 70^\circ$, and therefore the 1.2 solar radii upper limit should be close to the true value.

Table 1. System parameter of SDSS 1228+1040.

Distance	142 ± 15 pc
Effective temperature	22020 ± 200 K
White dwarf mass	$0.77 \pm 0.02 M_{\odot}$
White dwarf radius	$0.0111 \pm 0.003 R_{\odot}$
White dwarf cooling age	100 ± 5 Myr
Helium abundance	$\leq 0.1 \times \text{solar}$
Calcium abundance	$0.8 \pm 0.15 \times \text{solar}$
Progenitor mass	$4 - 5 M_{\odot}$
Progenitor main sequence life time	~ 70 Myr
Ca II full-width at zero intensity	1270 ± 35 km/s
Ca II peak separation	630 ± 5 km/s
Outer radius of the circumstellar disk	$\simeq 1.2 R_{\odot}$
Ellipticity	0.021

Supporting Online Material

1 A dynamical model for the emission of a rotating gas ring

The SDSS spectroscopy of the white dwarf SDSS1228+1040 presented in the main paper gave reasons to believe that the Ca II emission line profiles observed in the I -band are from a circumstellar gas disk. Here we outline the model we developed to fit the Ca II line profiles. It is apparent that there must be some form of asymmetry at work as the peaks of the line profiles are asymmetrical. The shape is very reminiscent of the “V/R” (violet/red) asymmetries seen in the emission line profiles of B-type emission line stars ($S1$ – $S3$). These are ascribed to a one-armed spiral wave which can be approximately modelled with a series of elliptical orbits. Drawing upon this analogy, we modelled the profiles of SDSS 1228+1040 by assuming that the orbits in the disk took the form of a series of co-aligned elliptical orbits of identical eccentricity. We further allowed the emission-line flux per unit area from the disk to vary as $1 + \epsilon \cos \theta$ where θ is the angle from periastron and ϵ is a measure of the asymmetry. A less obvious feature of the emission line profiles of Fig. 3 is that they are fainter at line centre relative to the double-peaks than can be explained by optically-thin line emission. That they are optically thick is also strongly suggested by the relatively equal line strengths within the Ca II triplet, even though Ca II 850 nm has only one tenth the oscillator strength of Ca II 854 nm. We therefore turned to the formalism of Horne & Marsh ($S4$) for optically thick line formation in which emission from any point in the disk takes on an azimuthal asymmetry owing to the local velocity shear, with strongest emission along the four directions at 45° to the radial direction and weakest emission in the radial direction and in the direction of gas flow. This has the effect of deepening the central dip between the line peaks. We had to modify the prescription of Horne & Marsh ($S4$) slightly to allow for elliptical as opposed to circular motion, although the effect overall was weak, since the ellipticity implied by the data was small.

Apart from an arbitrary normalisation factor, the following parameters were needed to specify the model fully: (a) $M_W = 0.75$, the mass of white dwarf which determines the relation between orbital radius and speed, (b) $e = 0.021$, the eccentricity, (c) the angle of the periastron to our line-of-sight, defined so that at 0° we look along the major-axes from peri- towards apastron, while at 90° we look along the minor axis with the periastron emission red-shifted, (d) inner semi-major axis $a_{in} = 0.64 R_\odot$, (e) outer semi-major axis $a_{out} = 1.2 R_\odot$, (f) exponent of the radial power law used to set the emissivity $\propto r^\alpha$ where $\alpha = -0.9$, (g) an optical depth parameter $Q' = 2.5$, analogous to the combination $Q \sin i \tan i$ from Horne & Marsh (*S4*). Since $Q \sim 1$, this suggests that the orbital inclination $i \sim 70^\circ$, and finally (h) the azimuthal asymmetry factor mentioned above with value $\epsilon = -0.19$. All parameters other than the mass of the white dwarf were allowed to vary. Experience from similar line profiles in cataclysmic variable stars suggests that systematic effects rather than statistical errors dominate, and the fit in this case, while qualitatively reasonable, is not a statistically good match to the data. Therefore we refrain from giving formal confidence intervals, but instead discuss which features in the data lead to constraints on these parameters to help the reader evaluate our model.

Apart from the allowance for optical depth, we made no allowance for inclination because its only effect is to scale the velocities in proportion to $\sin i$. This scaling can be counter-balanced by re-scaling the major-axis parameters a_{in} and a_{out} such that $a \propto \sin^2 i$. Thus the value of the outer semi-major axis $a_{out} = 1.2 R_\odot$, which is almost the outer radius since the eccentricity is small, is an upper limit to the real value. Since the optical depth parameter (which comes from the depth of central dip in the profiles) points to a large inclination, we believe this to be close to the true value, with a likely range of order 0.9 to $1.2 R_\odot$; this is quite robust as the outer major-axis limit is set by the velocities of the line peaks which are well-defined. An interesting feature of our model is that we also require a fairly large inner semi-major axis $a_{in} = 0.64 R_\odot$, which is subject to the same inclination uncertainties as a_{in} , but also additional uncertainty owing to

correlation with parameter (f), the emissivity power law exponent. The inner cut-off is required to fit the steep drop-off in the line wings; this presumably reflects an absence of emission rather than an absence of material given the presence of metals in the white dwarf’s photosphere. It could be caused, for instance, by ionisation of the Ca II ions close to the white dwarf.

The eccentricity, periastron angle and azimuthal asymmetry parameters are necessary because of the asymmetry of the profiles. The exact nature of the asymmetry is uncertain and thus we regard these parameters as the least reliable, although there is no doubt of the asymmetry. If our interpretation in terms of eccentric orbits contributing to a one-armed spiral is correct, further observations of the object are of considerable interest for we expect such orbits to precess. The asymmetries in Be stars precess within the distorted gravitational fields of the rapidly rotating stars for instance on decade-long timescales. The narrow photospheric Mg II absorption line shows that SDSS 1228+1040 is not rapidly rotating, but general relativity alone implies a precession rate of order 5° per year in the orientation of the outermost elliptical orbits, and pressure effects within the disk could contribute as well and may indeed be much more significant (S5). Such precession effects must be computed within the framework of fluid disk models since the precession rate is a strong function of radius and would be expected to randomise the orbit orientations if fluid effects were not taken into account; the Be stars are proof that it is possible for similar asymmetries to persist over long timescales (years to decades).

Our data do not directly constrain the thickness of the disk, but we can argue that it must be thin as follows: LTE (local thermodynamic equilibrium) models of the disk suggest a temperature of around 4500 to 5500 K for the disk. Any hotter and numerous metal lines that are not observed start to appear, while any colder and the Fe II lines disappear. The sound speed, assuming dominance by CNO elements in the absence of hydrogen and helium, is of order $C_S = 2 \text{ km s}^{-1}$. The thickness of the disk is then of order $H = (C_S/V_{\text{Orb}})R$ where V_{Orb} is the orbital velocity at radius R in the disk (S6) (6). This works out at $\sim 0.005 R_\odot$, comparable to

the size of the white dwarf. The same LTE models place a weak lower limit on the Ca II/H ratio which must be > 3 times solar; the data in hand are consistent with no hydrogen at all.

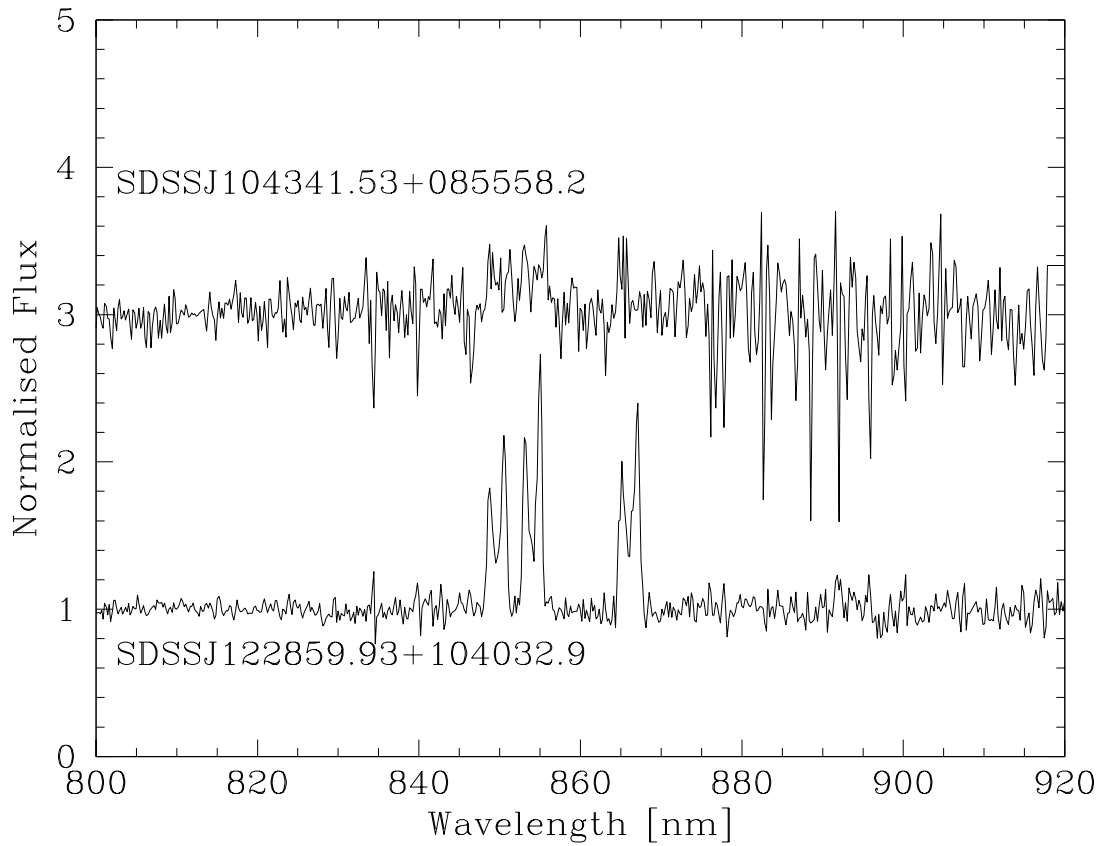
2 An investigation of white dwarfs in the SDSS

We have investigated all white dwarfs with hydrogen-dominated atmospheres brighter than $g = 17.5$ contained in Data Release 4 of the Sloan Digital Sky Survey (SDSS) (*S7*) (*7*) for signs of either photospheric metal absorption lines or Ca II emission in the *I*-band. Because the SDSS spectroscopy has a relatively low spectral resolution ($\lambda/\Delta\lambda \simeq 1800$), the detection of metal lines is limited to relatively high abundances such as observed in SDSS 1228+1040. We have not identified any additional white dwarf which exhibits significant metal absorption. The detection of Ca II emission with equivalent width comparable to the lines detected in SDSS 1228+1040 is robust for spectra in the considered magnitude range. However, we have identified only one additional white dwarf which shows flux excess in the region of the Ca II triplet (SDSS J104341.53+085558.2, Fig. S1). The equivalent width of the Ca II triplet in SDSS 1043+0855 is a factor three lower than in SDSS 1228+1040, and its SDSS spectrum suffers from strong residuals from imperfect night sky line subtraction in the *I*-band. A spectral fit to the SDSS spectrum of SDSS 1043+0855 results in a temperature of 18900 ± 300 K and a surface gravity of $\log g = 8.2 \pm 0.1$, similar to the parameters found for SDSS 1228+1040.

Circumstellar metal disks are most likely to be found around white dwarfs with substantial metal abundances. Published spectroscopy of known metal-polluted white dwarfs with temperatures in excess of 15 000 K does typically not cover the red end of the optical wavelength range (e.g. *S8*), and an assessment of the frequency of circumstellar gas disks will require a systematic survey of these stars.

References and Notes

1. A. T. Okazaki, *PASJ* **43**, 75 (1991).
2. A. Meilland, P. Stee, J. Zorec, S. Kanaan, *A&A* **455**, 953 (2006).
3. P. Stee, F. X. de Araujo, *A&A* **292**, 221 (1994).
4. K. Horne, T. R. Marsh, *MNRAS* **218**, 761 (1986).
5. G. I. Ogilvie, *MNRAS* **325**, 231 (2001).
6. J. E. Pringle, *ARA&A* **19**, 137 (1981).
7. D. J. Eisenstein, *et al.*, *ApJS* **in press**, [astro-ph/0606700](#) (2006).
8. B. Zuckerman, D. Koester, I. N. Reid, M. Hünsch, *ApJ* **596**, 477 (2003).



Supporting Figure 1. Normalised spectra of SDSS 1228+1040 and SDSS 1043+0855, the only other white dwarf among the brightest 406 hydrogen-dominated white dwarfs in Data Release 4 of the SDSS that exhibits excess emission in the region of the Ca II triplet. The spectrum of SDSS 1043+0855 has been offset by two units. The large amount of noise in the spectrum of SDSS 1043+0855 is due to imperfections in the removal of strong night sky lines.